J | P | S | T

http://jpst.irost.ir

Journal of Particle Science and Technology

IROST

Adsorption of CO_2 and SO_2 on multi-walled carbon nanotubes: experimental data and modeling using artificial neural network

Naghmeh Iraji[a], Mohammad Hojjat[a,*], Seyedfoad Aghamiri[a] , Mohammad Reza Talaie[a,b], Elham Molyanyan[a]

[a] *Department of Chemical Engineering, Faculty of Engineering, University of Isfahan, Isfahan, Iran*

[b] *Chemical Engineering Department, Faculty of Chemical, Oil and Gas Engineering, Shiraz University, Shiraz, Iran*

HIGHLIGHTS

- An experimental approach for CO_2 and SO_2 capturing by using multi-walled carbon nanotubes (MWCNT).
- Modification of MWCNTs via functionalization and then studied the effects of oxygen and nitrogen functional groups on the adsorption performance of the adsorbents.
- Designing an ANN model to predict the equilibrium adsorption of CO_2 and SO_2.
- Assessment of the ability of an artificial neural network model to predict adsorption experimental data.
- Comparison of ANN model with well-known adsorption isotherms.

GRAPHICAL ABSTRACT

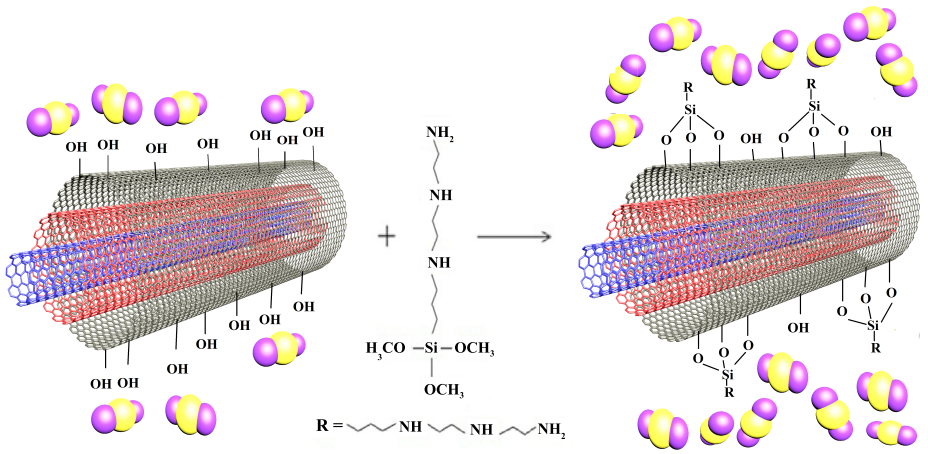

ARTICLE INFO

Article history:

Received 27 November 2018
Revised 22 January 2019
Accepted 29 January 2019

Keywords:

Adsorption
MWCNT
Isotherm carbon dioxide
Artificial neural network

ABSTRACT

Multi-walled carbon nanotubes (MWCNTs) containing hydroxylgroups (OH-MWCNT) were modified by functionalization with 3-[2-(2-aminoethylamino)ethylamino]propyl trimethoxysilane (TRI). Adsorption isotherms of pure CO_2 and SO_2 on the pristine MWCNT, OH-MWCNT, and amine functionalized MWCNT (amine-MWCNT) were measured at two temperatures of 313.2 K and 323.2 K and pressures up to 2.1 bar by a static volumetric method. Capacities of all three types of adsorbents for CO_2 adsorption are greater than those of CO_2. The performance of amine-MWCNT in adsorpting CO_2 is higher than the other two adsorbents. The average saturated capacity of amine-MWCNT for adsorption of pure CO_2 at 313.2 K are about 38.6% and 20.8% higher than OH-MWCNT and pristine-MWCNT, respectively. Corresponding values for adsorption of pure CO_2 are about 51.3% and 89.65%. Also, the equilibrium adsorption capacity of pristine MWCNT and amine-MWCNT for mixtures for CO_2, nitrogen, and water vapor at 299.2 K was obtained. The equilibrium adsorption of CO_2 increases as the water content increases in the presence of diluting gas (nitrogen). Freundlich and Langmuir equations were fitted on experimental adsorption isotherms. The Freundlich equation predicts experimental data better than the Langmuir equation. A multi-layer perceptron artificial neural network (ANN) model has been also proposed for predicting adsorption experimental data. The average and maximum difference between experimental data and values predicted by ANN model are about 3% and 24%, respectively.

* *Corresponding author: Tel.: +9831-37934074 ; Fax: +9831-37934031 ; E-mail address: m.hojjat@eng.ui.ac.ir*

DOI: 10.22104/JPST.2019.3317.1140

1. Introduction

Emission of greenhouse gases from fossil fuel combustion causes serious adverse effects on the environment including global warming and acid rains [1-5]. About 60% of the atmosphere temperature rise is attributed to carbon dioxide emission [6,7]. Another harmful product of fossil fuel combustion is SO_2, which is also considered an important air pollutant [8-11]. Absorption, adsorption, cryogenic, and membrane separation are potential methods for CO_2 capture [2, 3,5,12-18]; while, wet scrubbing and dry sorption processes are common technologies for SO_2 removal [9,10,19,20]. Adsorption on porous solid material such as carbon nanotubes (CNT) [21-23], activated carbons [10,17,18,24-28], zeolites [3,15,18,29-32], and MOFs [33-36] is a developing technology for removing gaseous pollutants. Effective application of adsorption strongly depends on the characteristics of the adsorbent such as good chemical and thermal stability, sufficient adsorption capacity, high selectivity, convenient regeneration and low cost [7,15,17,27,28,32,37-42]. Porous carbon materials have been proved to be effectively applicable in gas storage and separation. CNTs are a suitable choice among available carbon-based materials [18,43,44]. Due to their unique physical and chemical properties, MWCNTs have recently attracted a great deal of interest among researchers [23,45,46]. CNTs have the capability of removing a diversity of air pollutants [47,48]. Since external layers of CNTs are chemically inactive they are not generally desirable for specific applications [44,49,50]. Functionalization of carbon nanotubes is an effective method that improves their adsorption capacity [18, 51-53]. The functional groups containing oxygen and nitrogen atoms could be introduced on the surface of CNTs through chemical treatments. Insertion of amine groups on CNTs improves their catalytic activity and basicity which increases their adsorption capacity and selectivity of acid gases such as CO_2 and SO_2 [17, 54-57].

In recent years, data driven models based on experimental results, such as artificial neural network (ANN) and fuzzy logic, have been applied to find general models for adsorption equilibria and kinetics. Abdul Kareem *et al.* [58] measured supercritical CO_2 adsorption on 13X and 5A zeolites at two different temperature of 323.15 and 343.15 K (their experimental data modeled via ANN). Equilibrium data of carbon dioxide adsorption on activated carbon were modeled by using a multi-layer feed-forward neural network and compared with predicted values of Sips and Langmuir models by Rostami *et al.* [59]. They found that the efficiency and accuracy of the ANN model was significantly higher than the Sips and Langmuir models. In addition, unlike the Langmuir model, the neural network is not limited to isothermal conditions. Saucedo-Delgado *et al.* [60] had experimentally investigated the adsorption of fluoride from water on a protonated clinoptilolite. They also proposed a model on the basis of ANN, Langmuir and pseudo-second order equations. Results show that this hybrid model is in good agreement with the kinetics and isotherms experimental data. Modelling adsorption of dyes from aqueous solutions using ANN was also reviewed by Ghaedi and Vafaei [61].

In this research adsorption isotherms of CO_2 and SO_2 gases on three kinds of MWCNTs, i.e. pristine, hydroxylated, and amine functionalized MWCNTs, at two different temperatures of 313.2 K and 323.2 K are experimentally investigated and modeled by a simple single multi-layer perceptron ANN model. This may be the first step in finding models that have the ability to predict the behavior of multi-component adsorption systems. Also, two well-known Langmuir and Freundlich models were fitted on experimental data. These models were compared with the resulting ANN model.

2. Experimental methods

2.1. Materials

Specifications of materials used in the present work are shown in Table 1. All components have been used as received.

The SEM images of as received MWCNTs are shown in Fig. 1.

2.2. Amine functionalization of MWCNTs

MWCNTs were functionalized according to the method described in our previous work [62]. The OH-MWCNTs were first placed in an oven at 393.2 K for 2 h to dehydrate, then they were dispersed in 75 mL of toluene and stirred at room temperature for 30 min. After that 0.3 mL water was added to the mixture and sonicated for 10 min, then the suspension was stirred for 3 h. The temperature was increased to 358 K and

Table 1. Specifications and structural properties of used materials.

Component	Supplier	Purity (%)	Important Speciation
CO_2	Farafan Gas Company (Iran)	99.99	-
SO_2	Farafan Gas Company (Iran)	99.99	-
N_2	Farafan Gas Company (Iran)	99.99	-
TRI	Sigma-Aldrich	> 99.9	CAS No. 35141-30-1
Toluene	Merck Company	99	-
n-Hexane	Merck Company	99	-
Pristine MWCNT	Neunano Company	> 95	ID*: 2-5 nm
			OD**: <8 nm
			SSA***: > 500 m^2/g
OH-MWCNT	Neunano Company	> 95	ID: 2-5 nm
			OD: <8 nm
			SSA: > 500 m^2/g

*ID = Inner diameter, **OD = Outer diameter, ***SSA = Specific surface area

1.5 ml of TRI was added to the suspension and refluxed for 16 h. The resulting suspension was filtered, and the carbon nanotubes were washed with toluene and *n*-hexane and dried in an oven at 353 K for 2 h.

2.3. Characterization of MWCNTs

X-ray diffraction results (XRD, Bruker, D8, Germany) were used to investigate the structural characteristics of the CNTs. A qualitative analysis of the functional groups on modified MWCNTs was performed by FT-IR spectra (JASCO, Japan). Fig. 2 presents the XRD spectra of pristine-MWCNT, OH-MWCNT, and amine-MWCNT. Similar trends of plots indicated that the crystalline structure of the nanotubes is not affected by functionalization. The intensity of the C(002) peak of amine-MWCNTs is significantly less than that of OH-MWCNTs due to lower packing density of amine-MWCNTs and defects resulting from the functionalization [62,63].

The FT-IR spectra of MWCNTs are plotted in Fig. 3. In the spectra of OH-MWCNT and amine-MWCNT a

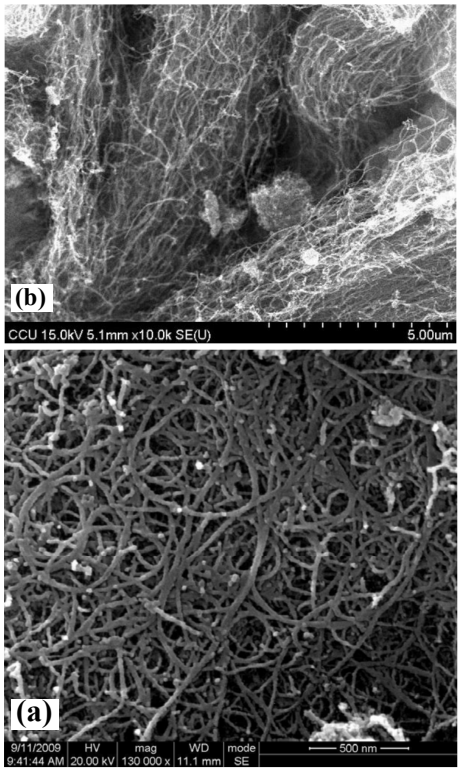

Fig. 1. SEM images of as received MWCNTs, a) pristine-MWCNT and b) OH-MWCNT.

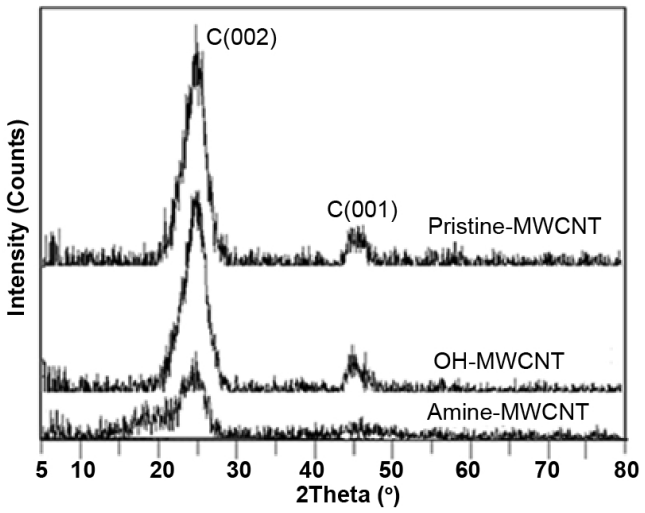

Fig. 2. XRD patterns of MWCNT, OH-MWCNT, and amine-MWCNT.

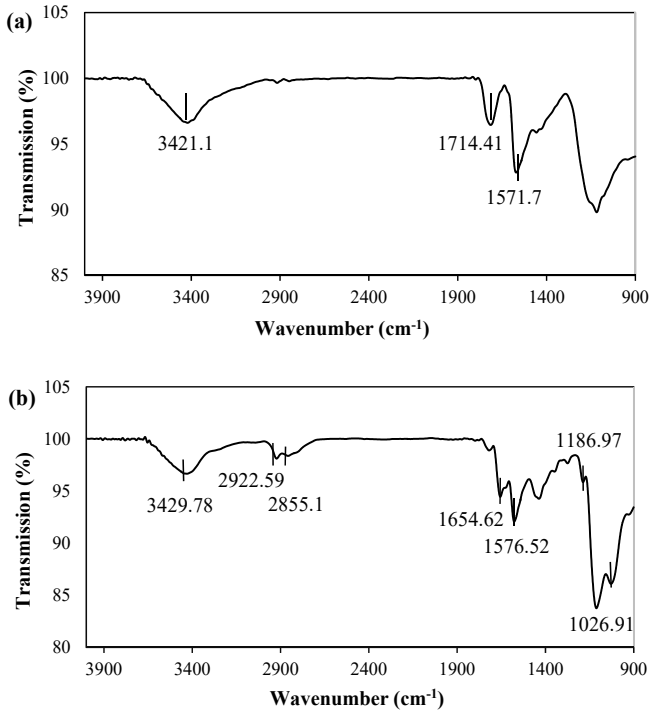

Fig. 3. FTIR spectra of (a) OH-MWCNT and (b) amine-MWCNT.

peak appears at 1571.7 and 1576.52 cm^{-1}, respectively, which is the result of C=C bonds in the nanotubes [6]. Due to the existence of hydroxyl (-OH) stretching vibration and C=O bonds two peaks appear at 3421 and 1714 cm^{-1}, respectively [6,64,65]. The presence of a COOH functional group causes these two peaks to appear simultaneously [6, 66].

The peak at 3429.78 cm^{-1} in the amine-MWCNT is the result of NH_2 stretch of amine group which overlaps with the stretching vibration of the hydroxyl group. As a result of asymmetric and symmetric stretching vibration of the methylene group after amine functionalization, two peak place at 2922.59 and 2855.1 cm^{-1} [65]. Peaks at 1654.62, 1186.97, and 1026.91 cm^{-1} can be attributed to N-H vibration, C-N bond stretching, and Si-O-Si vibration, respectively [18,65]. Therefore the FT-IR shows the existence of CH_2, NH_2, N-H, and Si-O-Si bonds after amine functionalization which confirms that TRI has been grafted on the surface of MWCNTs [18].

The thermogravimetric behavior of samples was studied by a Rheometric Scientific TGA, in which the heating rate was 10 °C/min in argon atmosphere, results are shown in Fig. 4. The pristine MWCNT and OH-MWCNT are thermally stable up to 800 °C but amine-MWCNT losses about 30% of its weight between 150 to 700 °C due to organic component (TRI) decomposition.

The existence of amine functional groups on modified adsorbents was evaluated by a CHNS elemental analyzer

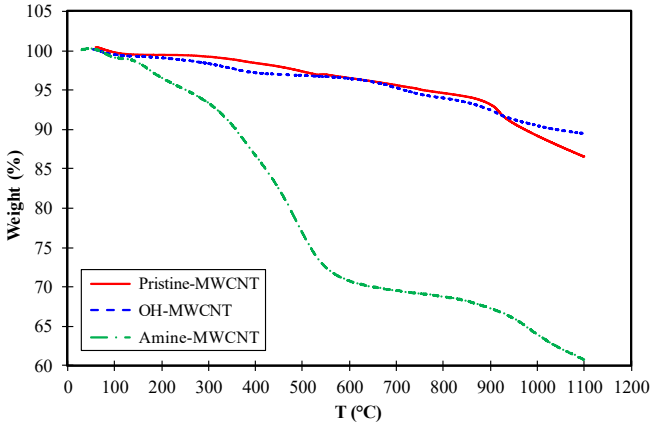

Fig. 4. TGA results of MWCNT, OH-MWCNT, and amine-MWCNT.

(LECO Co., 932). The CHNS elemental analysis of the nanotubes are shown in Table 2. The mass fraction of TRI in the functionalized adsorbent is about 31.6%, which is in accordance to TGA results.

2.4. Apparatus and procedure

2.4.1. Single-component gas adsorption

The amount of CO_2 and SO_2 adsorbed on MWCNTs were measured by the volumetric method. The experimental setup is shown in Fig. 5. It consisted of two cells adsorption and loading cells with volumes of 27.9752 and 75.2755 mL, respectively. The pressure in each cell was measured by a pressure transducer (M5156-11700X-070BG, Sensys Co., Korea) with an uncertainty of ±1 kPa. The temperature of the adsorption cell was controlled by a circulating system (Arian Azma Co., Iran) and measured by a PT-100 thermocouple with an accuracy of ± 0.1 K. The experiment is performed as follows:

A specific amount of the adsorbent was loaded in the adsorption cell, then the loading cell was filled by either CO_2 or SO_2 gases up to the desired pressure. After this, the captured gas in the loading cell is allowed

Table 2. Elemental analysis of OH-MWCNT and amine-MWCNT.

Element	Mass percent	
	OH-MWCNT	amine-MWCNT
Carbon	91.47	66.49
Hydrogen	0.35	4.03
Nitrogen	0.04	7.96
Sulfur	0.00	0.00

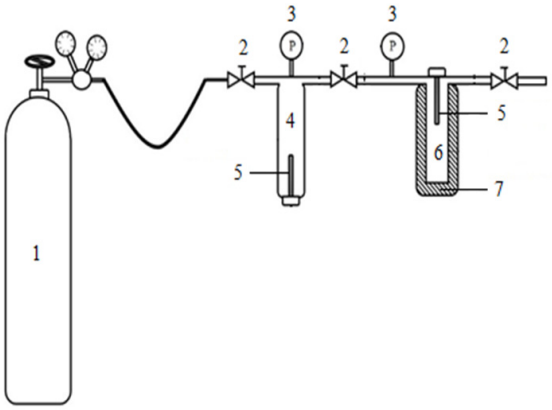

Fig. 5. Schematic diagram of the experimental apparatus; 1) gas storage, 2) valves, 3) pressure transducer, 4) loading cell 5) thermocouple, 6) adsorption cell and 7) circulating system.

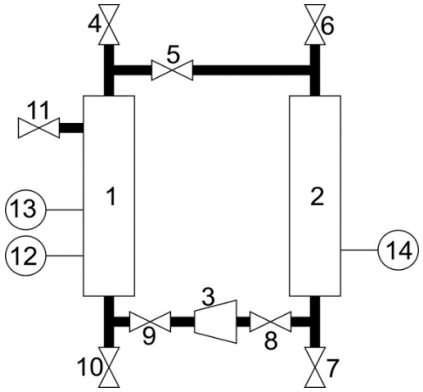

Fig. 6. Schematic diagram of closed loop volumetric apparatus: 1) loading cell, 2) Adsorption cell, 3) circulating pump, 4-10) ball valve, 11) needle valve, 12) temperature sensor, 13) pressure transmitter and 14) RTD temperature sensor.

to transfer to the adsorption cell up to an anticipated pressure while its temperature is remained constant. When equilibrium state was achieved, adsorption capacity was calculated by the Eq. (1).

$$\left(\frac{PV}{ZRT}\right)_{L_1} + \left(\frac{PV}{ZRT}\right)_{A_1} = \left(\frac{PV}{ZRT}\right)_{L_2} + \left(\frac{PV}{ZRT}\right)_{A_2} + NM \quad (1)$$

where P is the pressure, T is the temperature, V is the volume, R is the gas constant, M is the molecular weight, Z is the compressibility factor, and N is the amount of adsorption. Subscripts A and L refer to adsorption cell and load cell, respectively. Subscripts 1 and 2 also show adsorbent-loading state and final equilibrium state, respectively.

2.4.2. Mixtures adsorption

A closed-loop volumetric apparatus was employed to measure equilibrium adsorption of CO_2, from its mixture with nitrogen, in presence of water, as shown in Fig. 6. The volume of adsorption and loading cells were 1063.2198 and 703.6175 mL, respectively Pressure in the vessel was measured by a pressure transducer with an accuracy of ±0.1 kPa. In order to control the temperature, the adsorption cell was connected to a constant temperature bath (Arian Azma Co., Iran) which has the ability to maintain temperature uniformity within ±0.1 K. To obtain the adsorption isotherms, experimental apparatus was purged by nitrogen gas. The adsorbent was degassed by heating it up to 150 °C and then placing it in the adsorption cell. Valves 4, 5, 8 and 9 were open and the others were closed during both adsorbent loading and purging steps. After that, valve 4 was closed and pressure was increased to 1 bar gauge. In order to investigate the effect of moisture on the adsorption, nitrogen was dispersed in a water bath before mixing with pure CO_2 gas. Then valves 5 and 9 were closed and the loading cell was filled by a definite molar ratio of N_2 and CO_2 up to a total pressure the same as the pressure of the adsorption cell. Finally, valves 5 and 9 were opened and the circulating pump turned on. The change of pressure inside the adsorption cell was used to evaluate the amount of adsorbed gas.

2.5. Isotherm modeling

Two well-known models, Freundlich and Langmuir, were fitted on the experimental data. The Freundlich isotherm is presented as Eq. (2).

$$q = K_F (P)^{\frac{1}{n}} \quad (2)$$

where q is the equilibrium adsorption capacity, P is the equilibrium pressure, K_F is the Freundlich adsorption coefficient and n is a dimensionless constant which is an indication of the surface heterogeneity and is usually greater than unity [67-69]. The Langmuir model is given by the Eq. (3).

$$q = \frac{q_m (K_L P)}{1 + (K_L P)} \quad (3)$$

Where q_m is the saturation adsorption capacity and K_L is the adsorption equilibrium constant [70].

3. Artificial neural network design

ANN is a powerful tool inspired by the human nervous system which has the ability of modelling complex functions. An ANN consists of an input, an output, and one or more hidden layers. The number of hidden layers depends on the complexity of the studied system, but in most cases it is found that one or two hidden layers are sufficient [71-75]. Each layer consists of a number of neurons. The optimum number of neurons in the hidden layers is often determined by trial and errors.

The performance of ANNs can be assessed based on some statistical criteria, including mean squared error (MSE), maximum absolute relative deviation (Max ARD %), average absolute relative deviation (AARD %), and correlation coefficient (r), defined as:

$$MSE=\frac{1}{n}\sum_{i=1}^{n}\left(y_{iexp}-y_{ical}\right)^2 \tag{4}$$

$$Max\ ARD\ \% = Max_{i=1}^{n}\left(\left|\frac{y_{iexp}-y_{ical}}{y_{iexp}}\right|\times 100\right) \tag{5}$$

$$AARD\ \% = \frac{1}{n}\sum_{i=1}^{n}\left|\frac{y_{iexp}-y_{ical}}{y_{iexp}}\right|\times 100 \tag{6}$$

$$r=\frac{\sum_{i=1}^{n}\left[\left(y_{iexp}-\bar{y}_{exp}\right)\left(y_{ical}-\bar{y}_{cal}\right)\right]}{\sqrt{\sum_{i=1}^{n}\left(y_{iexp}-\bar{y}_{exp}\right)^2\sum_{i=1}^{n}\left(y_{ical}-\bar{y}_{cal}\right)^2}} \tag{7}$$

where y_{iexp}, y_{ical}, $\bar{y}$ and n are experimental data, predicted data by ANN, mean value of data, and number of data points, respectively.

4. Artificial neural network architecture

In present study a multi-layer perceptron neural network was designed to model the experimental data of CO_2 and SO_2 adsorption on pristine and functionalized MWCNTs.

First experimental data were normalized between 0 and 1 according to Eq. (8).

$$x_{i,norm}=\frac{x_i-x_{i,min}}{x_{i,max}-x_{i,min}} \tag{8}$$

Then the data was randomly divided into three parts; training data set (70%), validating data set (10%), and test data set (20%). The architecture of ANN was determined by trial and error.

The resulting ANN consists of three hidden layers each contains 10 neurons. The activation functions of all hidden layers are hyperbolic tangent sigmoid and that of the output layer is linear. The network is trained by Levenberg-Marquardt (LM) training algorithm. MSE (Eq. (4)) was chosen as the network performance criteria. ANN receives pressure, temperature, critical temperature and pressure of adsorbate, and a number as the character of adsorbent as input parameters and gives the amount of adsorbed gas as output.

5. Results and discussion

5.1. Artificial neural network

Fig. 7 shows the ANN predicted values of adsorption capacity against the experimental data. As can be seen there exists very good agreement between the experimental data and the corresponding values predicted by the ANN model. The values of statistical criteria are given in Table 3, suggesting the accuracy of proposed ANN.

5.2. Adsorption isotherms

Adsorption isotherms of pure SO_2 and CO_2 on pristine MWCNT, OH-MWCNT, and amine-MWCNT at 313.2 and 323.2 K are shown in Fig. 8 (a-c). As expected, for both gases adsorption capacity decreases as the temperature rises. Adsorption isotherms of SO_2 are more sensitive to temperature than those of CO_2. It is also observed that adsorption capacity for SO_2 is higher than CO_2 for all adsorbents over the entire temperature and pressure ranges. This can be explained by higher multipole moments and polarizability of SO_2 compared with CO_2 which in turn leads to stronger affinity of SO_2 with CNTs than CO_2 [37]. Nickmand *et al.* [76] obtained the same result using the Monte Carlo molecular simulation. As can be seen in Fig. 8(a), all isotherms are almost linear, which may be an indicator of a lack of active sites on pristine MWCNT. Fig. 8(b) shows that OH-MWCNT possesses higher adsorption

Table 3. Statistical criteria of proposed ANN.

	Max ARD %	AARD %	r
Training data	23.86	2.81	0.9984
Validating data	13.24	3.06	0.9971
Test data	17.88	3.74	0.9938

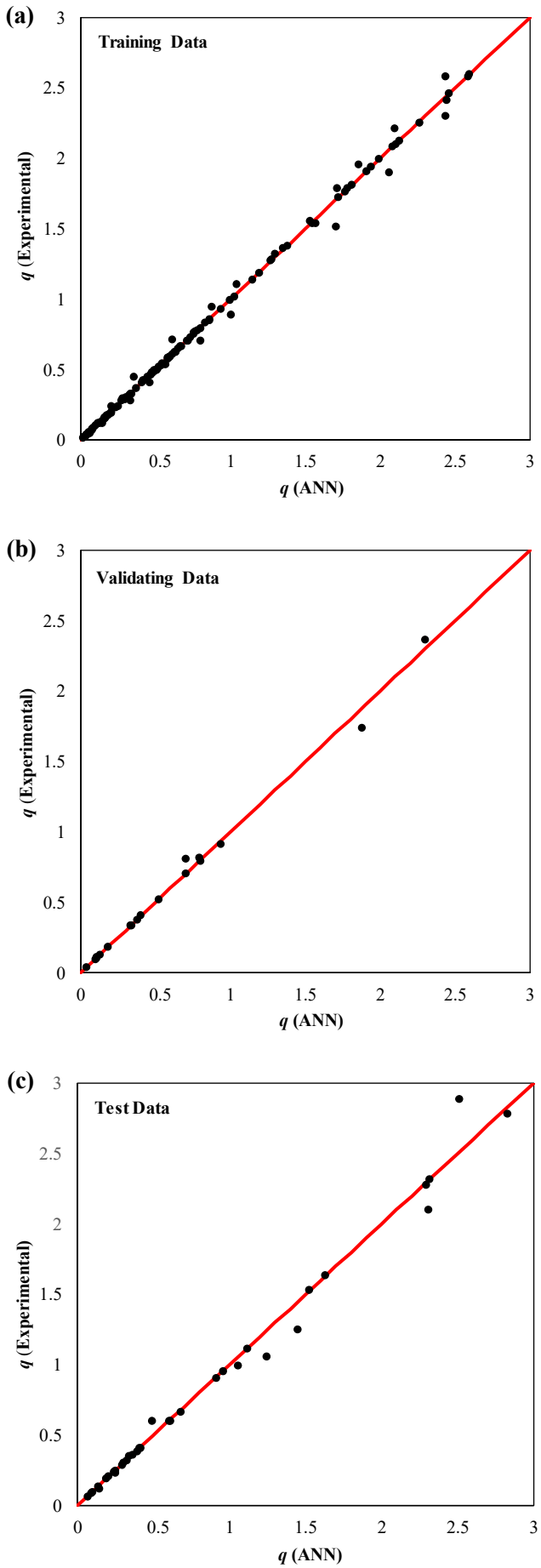

Fig. 7. ANN predicted q against experimental values of q (a) training data, (b) validating data, and (c) test dataset.

capacity than pristine MWCNT. This may be attributed to the functional groups and existence of active sites on the surface of OH-MWCNT.

Fig. 8(c) shows that the initial slopes of isotherms increased sharply which indicates active sites are created on the adsorbent during the functionalization step. Existence of functional groups on MWCNTs causes the adsorption capacity to increases, especially for SO_2 at low pressures. At low pressures, adsorption

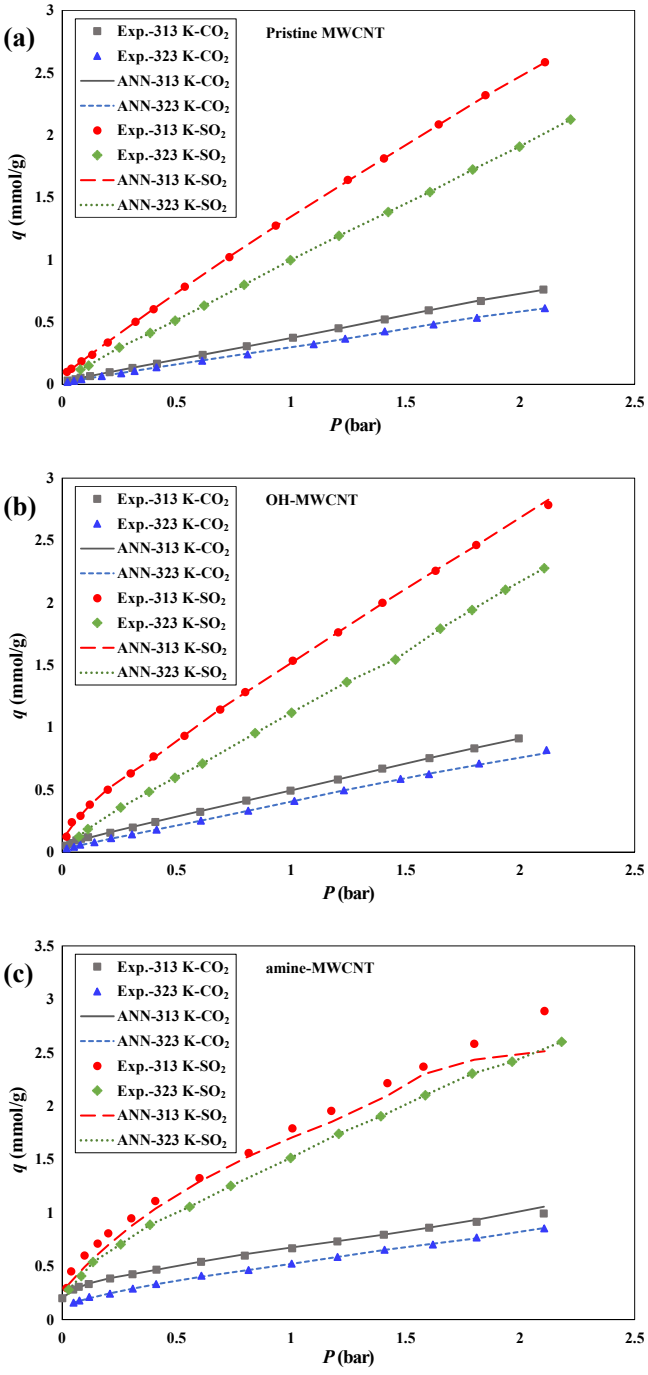

Fig. 8. Adsorption isotherms for CO_2 and SO_2 at 313.2 and 323.2 K (a) on pristine MWCNT, (b) on OH-MWCNT, and (c) on amine-MWCNT.

on MWCNTs is affected by the fluid-adsorbent interaction; therefore, functional groups led to increase fluid-adsorbent interactions. But at higher pressures, fluid-fluid interactions become more important than fluid-adsorbent interactions and the role of functional groups is reduced. This is in agreement with the results of a molecular simulation carried out by Nikmand *et al.* [76].

Predicted values of equilibrium adsorption by artificial neural network are also indicated in Fig. 8. It is clear that predicted values of ANN are in a good agreement with experimental data. The average and maximum difference between experimental data and those predicted by ANN are about 3% and 24%, respectively.

In Fig. 9 adsorption of CO_2 and SO_2 on three different adsorbents at 313.2 K is compared. It is observed that OH-MWCNT has a higher adsorption capacity than pristine MWCNT for both gases. Since the carbon atom in CO_2 has a non-bonded pair of electrons, electron-donor functional (hydroxyl) groups are able to increase CO_2 adsorption tendency. According to this figure amine-MWCNT demonstrates the best performance for both CO_2 and SO_2 adsorption especially at low pressures. This capability stems from the interaction between adsorbate gases and amine groups. However, this capability is played down at high pressures, this can be ascribed to the fact that at higher pressures the functional groups are entirely covered by adsorbate molecules.

The effect of humidity on adsorption behavior of both pristine MWCNT and amine-MWCNT at 299 K and 1 bar is shown in Fig. 10. The adsorbing gas was a mixture of $CO_2/N_2/H_2O$ containing 15 mol% of CO_2. This figure indicates that adsorption of CO_2 on both adsorbents increases with increasing relative humidity (RH). The ratio of adsorption capacities of amine-MWCNT to pristine-MWCNT decreases as the relative humidity increases. As explained by Su *et al.* [18] this observation may be justified by two reasons. First, CO_2 can be dissolved in the water adsorbed on the surface of MWCNTs. Second, the carbonate ion that resulted from the reaction between CO_2 and surface amine groups may form bicarbonate (HCO_3^-) as a result of further reaction with CO_2 and H_2O. A direct reaction between amine groups CO_2 and H_2O that forms HCO_3^- is also possible. The decrease in the slope of CO_2 adsorption taking place at high RHs could be attributed to competitive adsorption of CO_2 and H_2O at the same sorption site of adsorbents. Fig. 11 indicates the water adsorption isotherms for both adsorbents in the same conditions of Fig. 10. It is observed that the capacity of functionalized MWCNT is higher than that of pristine MWCNT.

5.3. Isotherms parameters

Tables 4 and 5 show the fitted parameters of Freundlich and Langmuir equations for adsorption isotherms of CO_2 and SO_2, respectively. It is observed that

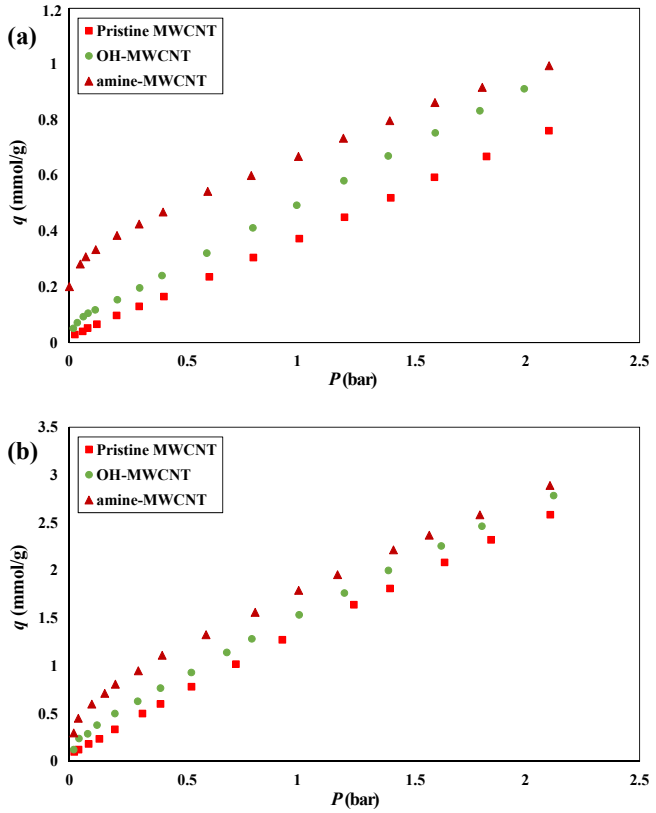

Fig. 9. Adsorption isotherms of a) CO_2, and b) SO_2 on pristine MWCNT, OH-MWCNT and amine-MWCNT at 313.2 K.

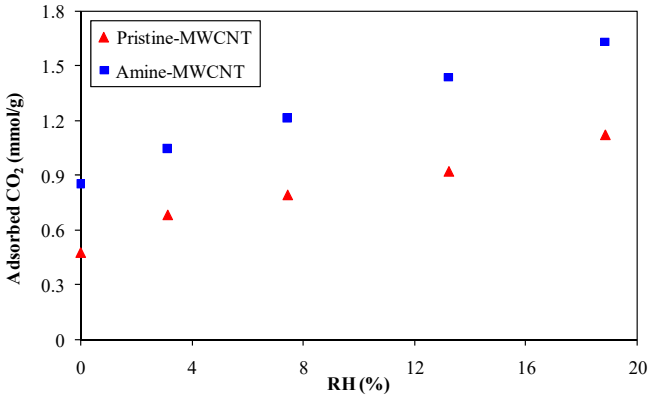

Fig. 10. The effect of relative humidity on CO_2 adsorption by MWCNTs at 299.2 K, mixture contains 15% CO_2.

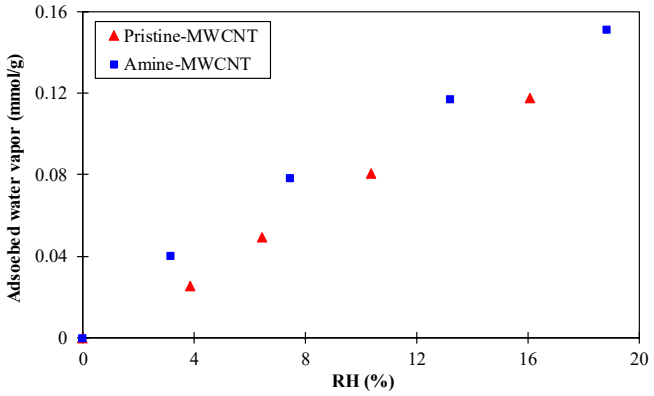

Fig.11. Adsorption isotherms of water vapor in presence of CO_2 and N_2 at 299.2 K, mixture contains 15% CO_2.

the parameter n in the Freundlich model (Eq. (2)) of amine-MWCNT for both gases is significantly greater than unity, which means that the isotherms have a nonlinear nature, and the surface is highly nonhomogeneous. The parameter k_L in the Langmuir model (Eq. (3)) of amine-MWCNT, especially for SO_2, is higher than that of other MWCNTs, which implies a strong bond between gas molecules and adsorbent due to existence of amine groups.

The Freundlich equation is in better agreement with the experimental data than the Langmuir equation. For amine-MWCNT, this is evidence that the heterogeneity of amine-MWCNT surface increases as a result of functionalization. The AARD% of predicted values of the artificial neural network are also presented for comparison. It is evident that the ability of ANN to predict experimental data is much better than that of the Freundlich and Langmuir models. In addition, ANN is not restricted to isothermal conditions.

6. Conclusion

The surface of MWCNT was modified through functionalization with TRI. The adsorption equilibrium isotherms of SO_2 and CO_2 on pristine MWCNT, OH-MWCNT, and amine-MWCNT were obtained at two different temperatures of 313.2 and 323.2 K. The adsorption capacity of SO_2 was higher than CO_2

Table 4. Parameters of Freundlich and Langmuir isotherms of CO_2 adsorption on MWCNTs.

Models	Parameters	Pristine MWCNT		OH-MWCNT		amine-MWCNT	
		313.2 K	323.2 K	313.2 K	323.2 K	313.2 K	323.2 K
Freundlich	k_F (mmol/g)/(bar$^{1/n}$)	0.3813	0.3043	0.5140	0.4106	0.7064	0.5522
	n	1.0833	1.0686	1.2528	1.0810	1.8370	1.6326
	R^2	0.9990	0.9991	0.9957	0.9991	0.9612	0.9883
	AARD %	10.6	9.0	14.9	10.4	11.0	6.9
Langmuir	q_m (mmol/g)	7.2045	6.5472	3.2464	6.1402	1.0285	1.1254
	k_L (1/bar)	0.0558	0.0487	0.1893	0.0718	2.6015	1.0591
	R^2	0.9990	0.9991	0.995	0.999	0.9007	0.9578
	AARD %	13.7	12	22.2	14	22.2	16.9
ANN	AARD %	1.3	1.7	3.6	2.1	1.5	1.1

Table 5. Parameters of Freundlich and Langmuir isotherms of SO_2 adsorption on MWCNTs.

Models	Parameters	Pristine MWCNT		OH-MWCNT		amine-MWCNT	
		313.2 K	323.2 K	313.2 K	323.2 K	313.2 K	323.2 K
Freundlich	k_F (mmol/g)/(bar$^{1/n}$)	1.3538	0.9988	1.5564	1.1302	1.8469	1.5833
	n	1.1540	1.0686	1.3239	1.0810	2.7055	1.9213
	R^2	0.9996	0.9997	0.9981	0.9989	0.9935	0.9960
	AARD %	6.7	3.3	8.5	4.5	7.1	6.5
Langmuir	q_m (mmol/g)	11.8454	20	7.3461	20	3.9647	4.4329
	k_L (1/bar)	0.1307	0.05276	0.2750	0.06002	0.9539	0.5848
	R^2	0.9993	0.9994	0.9953	0.9989	0.9726	0.9856
	AARD %	12.3	5.0	17.2	6.7	19.4	16.2
ANN	AARD %	0.9	1.1	2.7	2.0	8.3	10.0

for three kinds of adsorbents in the following order amine-MWCNT > OH-MWCNT > pristine MWCNT at both of temperatures. The adsorption capacity of CO_2 on pristine MWCNT, OH-MWCNT, and amine-MWCNT at 313.2 K and 0.2 bar are 0.098, 0.154, and 0.385 mmol/g, respectively, and for SO_2 are 0.336, 0.5, and 0.808 mmol/g, respectively. Results show that adsorption capacity is significantly improved through functionalization with amine, especially at low pressures. The effect of relative humidity (0-20 %) on CO_2 adsorption by pristine MWCNT and amine-MWCNT were also investigated. It is observed that the CO_2 adsorption increases by increase in RH. The two well-known isotherms, Freundlich and Langmuir, equations were fitted on experimental data. A multi-layer perceptron artificial neural network has been developed to predict the equilibrium adsorption of CO_2 and SO_2 on MWCNTs. The average and maximum differences between predicted values and experimental data are about 3 and 24%, respectively. A single ANN model was capable o the equilibrium adsorption of both adsorbates on all adsorbents at all temperatures with much higher accuracy than Freundlich and Langmuir models.

References

[1] J.L. Shelton, J.C. McIntosh, A.G. Hunt, T.L. Beebe, A.D. Parker, P.D. Warwick, R.M. Drake, J.E. McCray, Determining CO_2 storage potential during miscible CO_2 enhanced oil recovery: Noble gas and stable isotope tracers, Int. J. Greenh. Gas Con. 51 (2016) 239-253.

[2] M. Anas, A.G. Gönel, S.E. Bozbag, C. Erkey, Thermodynamics of adsorption of carbon dioxide on various aerogels, J. CO_2 Util. 21 (2017) 82-88.

[3] Y. Wang, T. Du, Y. Song, S. Che, X. Fang, L. Zhou, Amine-functionalized mesoporous ZSM-5 zeolite adsorbents for carbon dioxide capture, Solid State Sci. 73 (2017) 27-35.

[4] A. Alonso, J. Moral-Vico, A. Abo Markeb, M. Busquets-Fité, D. Komilis, V. Puntes, A. Sánchez, X. Font, Critical review of existing nanomaterial adsorbents to capture carbon dioxide and methane, Sci. Total Environ. 595 (2017) 51-62.

[5] C. Alonso-Moreno, S. García-Yuste, Environmental potential of the use of CO_2 from alcoholic fermentation processes. The CO_2-AFP strategy, Sci. Total Environ. 568 (2016) 319-326.

[6] S. Fatemi, M. Vesali-Naseh, M. Cyrus, J. Hashemi, Improving CO_2/CH_4 adsorptive selectivity of carbon nanotubes by functionalization with nitrogen-containing groups, Chem. Eng. Res. Des. 89 (2011) 1669-1675.

[7] A. Sayari, Y. Belmabkhout, R. Serna-Guerrero, Flue gas treatment via CO_2 adsorption, Chem. Eng. J. 171 (2011) 760-774.

[8] W. Wang, X. Peng, D. Cao, Capture of trace sulfur gases from binary mixtures by single-walled carbon nanotube arrays: A molecular simulation study, Environ. Sci. Technol. 45 (2011) 4832-4838.

[9] Q. Zhang, Q. Tao, H. He, H. Liu, S. Komarneni, An efficient SO_2-adsorbent from calcination of natural magnesite, Ceram. Int. 43 (2017) 12557-12562.

[10] J.M. Rosas, R. Ruiz-Rosas, J. Rodríguez-Mirasol, T. Cordero, Kinetic study of SO_2 removal over lignin-based activated carbon, Chem. Eng. J. 307 (2017) 707-721.

[11] J. Li, A. Woodward, X.-Y. Hou, T. Zhu, J. Zhang, H. Brown, J. Yang, R. Qin, J. Gao, S. Gu, J. Li, L. Xu, X. Liu, Q. Liu, Modification of the effects of air pollutants on mortality by temperature: A systematic review and meta-analysis, Sci. Total Environ. 575 (2017) 1556-1570.

[12] B. Wang, Z.H. Gan, Feasibility analysis of cryocooler based small scale CO_2 cryogenic capture. Comment on "Energy analysis of the cryogenic CO_2 process based on Stirling coolers" Song CF, Kitamura Y, Li SH [Energy, 2014 6(5) 580-89], Energy, 68 (2014) 1000-1003.

[13] G. Zhao, B. Aziz, N. Hedin, Carbon dioxide adsorption on mesoporous silica surfaces containing amine-like motifs, Appl. Energ. 87 (2010) 2907-2913.

[14] S.-C. Hsu, C. Lu, F. Su, W. Zeng, W. Chen, Thermodynamics and regeneration studies of CO_2 adsorption on multiwalled carbon nanotubes, Chem. Eng. Sci. 65 (2010) 1354-1361.

[15] R. Girimonte, B. Formisani, F. Testa, Adsorption of CO_2 on a confined fluidized bed of pelletized 13X zeolite, Powder Technol. 311 (2017) 9-17.

[16] A. Arefi Pour, S. Sharifnia, R. Neishabori Salehi, M. Ghodrati, Adsorption separation of CO_2/CH_4 on the synthesized NaA zeolite shaped with montmorillonite clay in natural gas purification process, J. Nat. Gas. Sci. Eng. 36 (2016) 630-643.

[17] Y. Kong, L. Jin, J. Qiu, Synthesis, characterization,

and CO_2 capture study of micro-nano carbonaceous composites, Sci. Total Environ. 463-464 (2013) 192-198.

[18] F. Su, C. Lu, W. Cnen, H. Bai, J.F. Hwang, Capture of CO_2 from flue gas via multiwalled carbon nanotubes, Sci. Total Environ. 407 (2009) 3017-3023.

[19] T. Kopaç, S. Kocabaş, Adsorption equilibrium and breakthrough analysis for sulfur dioxide adsorption on silica gel, Chem. Eng. Process. 41 (2002) 223-230.

[20] Y. Lv, X. Yu, S.-T. Tu, J. Yan, E. Dahlquist, Experimental studies on simultaneous removal of CO_2 and SO_2 in a polypropylene hollow fiber membrane contactor, Appl. Energ. 97 (2012) 283-288.

[21] M.M. Gui, Y.X. Yap, S.-P. Chai, A.R. Mohamed, Multi-walled carbon nanotubes modified with (3-aminopropyl)triethoxysilane for effective carbon dioxide adsorption, Int. J. Greenh. Gas Con. 14 (2013) 65-73.

[22] P. Kowalczyk, R. Holyst, Efficient Adsorption of Super Greenhouse Gas (Tetrafluoromethane) in Carbon Nanotubes, Environ. Sci. Technol. 42 (2008) 2931-2936.

[23] A. Reyhani, S.Z. Mortazavi, S. Mirershadi, A.N. Golikand, A.Z. Moshfegh, H2 adsorption mechanism in Mg modified multi-walled carbon nanotubes for hydrogen storage, Int. J. Hydrogen Energ. 37 (2012) 1919-1926.

[24] A. Somy, M.R. Mehrnia, H.D. Amrei, A. Ghanizadeh, M. Safari, Adsorption of carbon dioxide using impregnated activated carbon promoted by Zinc, Int. J. Greenh. Gas Con. 3 (2009) 249-254.

[25] V. Gaur, A. Sharma, N. Verma, Preparation and characterization of ACF for the adsorption of BTX and SO_2, Chem. Eng. Process. 45(1) (2006) 1-13.

[26] X. Zhou, H. Yi, X. Tang, H. Deng, H. Liu, Thermodynamics for the adsorption of SO_2, NO and CO_2 from flue gas on activated carbon fiber, Chem. Eng. J. 200 (2012) 399-404.

[27] A.I. Sarker, A. Aroonwilas, A. Veawab, Equilibrium and kinetic behaviour of CO_2 adsorption onto zeolites, carbon molecular sieve and activated carbons, Energy Proced. 114 (2017) 2450-2459.

[28] P. Ammendola, F. Raganati, R. Chirone, CO_2 adsorption on a fine activated carbon in a sound assisted fluidized bed: Thermodynamics and kinetics, Chem. Eng. J. 322 (2017) 302-313.

[29] Z. Zhao, X. Cui, J. Ma, R. Li, Adsorption of carbon dioxide on alkali-modified zeolite 13X adsorbents, Int. J. Greenh. Gas Con. 1 (2007) 355-359.

[30] S. Cavenati, C.A. Grande, A.E. Rodrigues, Adsorption equilibrium of methane, carbon dioxide, and nitrogen on zeolite 13X at high pressures, J. Chem. Eng. Data 49 (2004) 1095-1101.

[31] D. Saha, Z. Bao, F. Jia, S. Deng, Adsorption of CO_2, CH_4, N_2O, and N_2 on MOF-5, MOF-177, and zeolite 5A, Environ. Sci. Technol. 44 (2010) 1820-1826.

[32] F. Gholipour, M. Mofarahi, Adsorption equilibrium of methane and carbon dioxide on zeolite 13X: Experimental and thermodynamic modeling, J. Supercrit. Fluid. 111 (2016) 47-54.

[33] S. Basu, A. Cano-Odena, I.F.J. Vankelecom, MOF-containing mixed-matrix membranes for CO_2/CH_4 and CO_2/N_2 binary gas mixture separations, Sep. Purif. Technol. 81 (2011) 31-40.

[34] R. Sabouni, H. Kazemian, S. Rohani, Mathematical modeling and experimental breakthrough curves of carbon dioxide adsorption on metal organic framework CPM-5, Environ. Sci. Technol. 47 (2013) 9372-9380.

[35] Y. Wu, L. Wei, H. Wang, L. Chen, Q. Zhang, First principles study of enhanced CO_2 adsorption on MOF-253 by salt-insertion, Comp. Mater. Sci. 111 (2016) 79-85.

[36] H. Wu, C.G. Thibault, H. Wang, K.A. Cychosz, M. Thommes, J. Li, Effect of temperature on hydrogen and carbon dioxide adsorption hysteresis in an ultramicroporous MOF, Micropor. Mesopor. Mat. 219 (2016) 186-189.

[37] H. Deng, H. Yi, X. Tang, Q. Yu, P. Ning, L. Yang, Adsorption equilibrium for sulfur dioxide, nitric oxide, carbon dioxide, nitrogen on 13X and 5A zeolites, Chem. Eng. J. 188 (2012) 77-85.

[38] M.G. Plaza, C. Pevida, B. Arias, J. Fermoso, F. Rubiera, J.J. Pis, A comparison of two methods for producing CO_2 capture adsorbents, Energy Proced. 1 (2009) 1107-1113.

[39] M.G. Plaza, C. Pevida, A. Arenillas, F. Rubiera, J.J. Pis, CO_2 capture by adsorption with nitrogen enriched carbons, Fuel, 86 (2007) 2204-2212.

[40] G.P. Lithoxoos, A. Labropoulos, L.D. Peristeras, N. Kanellopoulos, J. Samios, I.G. Economou, Adsorption of N_2, CH_4, CO and CO_2 gases in single walled carbon nanotubes: A combined experimental and Monte Carlo molecular simulation study, J. Supercrit. Fluid. 55 (2010) 510-523.

[41] S.J. Allen, E. Ivanova, B. Koumanova, Adsorption of sulfur dioxide on chemically modified natural clinoptilolite. Acid modification, Chem. Eng. J. 152 (2009) 389-395.

[42] M.G. Plaza, I. Durán, F. Rubiera, C. Pevida, Adsorption-based process modelling for post-combustion CO_2 capture, Energy Proced. 114 (2017) 2353-2361.

[43] X. Peng, D. Cao, W. Wang, Adsorption and separation of $CH_4/CO_2/N_2/H_2/CO$ mixtures in hexagonally ordered carbon nanopipes CMK-5, Chem. Eng. Sci. 66 (2011) 2266-2276.

[44] X. Ren, C. Chen, M. Nagatsu, X. Wang, Carbon nanotubes as adsorbents in environmental pollution management: A review, Chem. Eng. J. 170 (2011) 395-410.

[45] I. Bertóti, I. Mohai, M. Mohai, J. Szépvölgyi, Surface modification of multi-wall carbon nanotubes by nitrogen attachment, Diam. Relat. Mater. 20 (2011) 965-968.

[46] C. Chen, J. Hu, D. Shao, J. Li, X. Wang, Adsorption behavior of multiwall carbon nanotube/iron oxide magnetic composites for Ni(II) and Sr(II), J. Hazard. Mater. 164 (2009) 923-928.

[47] R.Q. Long, R.T. Yang, Carbon nanotubes as superior sorbent for dioxin removal, J. Am. Chem. Soc. 123 (2001) 2058-2059.

[48] S. Agnihotri, M.J. Rood, M. Rostam-Abadi, Adsorption equilibrium of organic vapors on single-walled carbon nanotubes, Carbon, 43 (2005) 2379-2388.

[49] M.D. Ganji, A. Bakhshandeh, Functionalized single-walled carbon nanotubes interacting with glycine amino acid: DFT study, Physica B, 406 (2011) 4453-4459.

[50] E. Dilonardo, M. Penza, M. Alvisi, C. Di Franco, R. Rossi, F. Palmisano, L. Torsi, N. Cioffi, Electrophoretic deposition of Au NPs on MWCNT-based gas sensor for tailored gas detection with enhanced sensing properties, Sensor. Actuat. B-Chem. 223 (2016) 417-428.

[51] Y.-j. Xu, A. Rosa, X. Liu, D.-s. Su, Characterization and use of functionalized carbon nanotubes for the adsorption of heavy metal anions, New Carbon Mater. 26 (2011) 57-62.

[52] R. Ben-Mansour, M.A. Habib, O.E. Bamidele, M. Basha, N.A.A. Qasem, A. Peedikakkal, T. Laoui, M. Ali, Carbon capture by physical adsorption: Materials, experimental investigations and numerical modeling and simulations – A review, Appl. Energ. 161 (2016) 225-255.

[53] M. Kah, X. Zhang, T. Hofmann, Sorption behavior of carbon nanotubes: Changes induced by functionalization, sonication and natural organic matter, Sci. Total Environ. 497-498 (2014) 133-138.

[54] E. Raymundo-Piñero, D. Cazorla-Amorós, A. Linares-Solano, The role of different nitrogen functional groups on the removal of SO_2 from flue gases by N-doped activated carbon powders and fibres, Carbon, 41 (2003) 1925-1932.

[55] S. Maldonado, S. Morin, K.J. Stevenson, Structure, composition, and chemical reactivity of carbon nanotubes by selective nitrogen doping, Carbon, 44 (2006) 1429-1437.

[56] S. Kundu, W. Xia, W. Busser, M. Becker, D.A. Schmidt, M. Havenith, M. Muhler, The formation of nitrogen-containing functional groups on carbon nanotube surfaces: a quantitative XPS and TPD study, Phys. Chem. Chem. Phys. 12 (2010) 4351-4359.

[57] C. Chen, Y. Huang, Enhanced photoreactivity of amine-functionalized carbon nanotubes under sunlight in the aquatic environment, Sci. Total Environ. 636 (2018) 1577-1584.

[58] F.A. Abdul Kareem, A.M. Shariff, S. Ullah, F. Dreisbach, L.K. Keong, N. Mellon, S. Garg, Experimental measurements and modeling of supercritical CO_2 adsorption on 13X and 5A zeolites, J. Nat. Gas. Sci. Eng. 50 (2018) 115-127.

[59] A. Rostami, M.A. Anbaz, H.R. Erfani Gahrooei, M. Arabloo, A. Bahadori, Accurate estimation of CO2 adsorption on activated carbon with multi-layer feed-forward neural network (MLFNN) algorithm, Egypt. J. Petrol. 27 (2017) 65-73.

[60] B.G. Saucedo-Delgado, D.A. De Haro-Del Rio, L.M. González-Rodríguez, H.E. Reynel-Ávila, D.I. Mendoza-Castillo, A. Bonilla-Petriciolet, J. Rivera de la Rosa, Fluoride adsorption from aqueous solution using a protonated clinoptilolite and its modeling with artificial neural network-based equations, J. Fluorine Chem. 204 (2017) 98-106.

[61] A.M. Ghaedi, A. Vafaei, Applications of artificial neural networks for adsorption removal of dyes from aqueous solution: A review, Adv. Colloid Interf. Sci. 245 (2017) 20-39.

[62] E. Molyanyan, S. Aghamiri, M.R. Talaie, N. Iraji, Experimental study of pure and mixtures of CO_2 and

CH_4 adsorption on modified carbon nanotubes, Int. J. Environ. Sci. Technol. 13 (2016) 2001-2010.

[63] L. Chen, H. Xie, Y. Li, W. Yu, Surface chemical modification of multiwalled carbon nanotubes by a wet-mechanochemical reaction, J. Nanomater. 2008 (2008) 783981.

[64] L. Niu, Y. Luo, Z. Li, A highly selective chemical gas sensor based on functionalization of multi-walled carbon nanotubes with poly(ethylene glycol), Sensor. Actuat. B-Chem. 126 (2007) 361-367.

[65] G. Vuković, A. Marinković, M. Obradović, V. Radmilović, M. Čolić, R. Aleksić, P.S. Uskoković, Synthesis, characterization and cytotoxicity of surface amino-functionalized water-dispersible multi-walled carbon nanotubes, Appl. Surf. Sci. 255 (2009) 8067-8075.

[66] G.D. Vuković, A.D. Marinković, M. Čolić, M.Đ. Ristić, R. Aleksić, A.A. Perić-Grujić, P.S. Uskoković, Removal of cadmium from aqueous solutions by oxidized and ethylenediamine-functionalized multi-walled carbon nanotubes, Chem. Eng. J. 157 (2010) 238-248.

[67] Duong D. Do, Adsorption analysis: equilibria and kinetics, Imperial College Press, London, 1998.

[68] X. Li, H. Liu, D. Luo, J. Li, Y. Huang, H. Li, Y. Fang, Y. Xu, L. Zhu, Adsorption of CO_2 on heterostructure $CdS(Bi_2S_3)/TiO_2$ nanotube photocatalysts and their photocatalytic activities in the reduction of CO_2 to methanol under visible light irradiation, Chem. Eng. J. 180 (2012) 151-158.

[69] S. Zhang, T. Shao, S.S.K. Bekaroglu, T. Karanfil, The impacts of aggregation and surface chemistry of carbon nanotubes on the adsorption of synthetic organic compounds, Environ. Sci. Technol. 43 (2009) 5719-5725.

[70] Y.C. Chiang, P.Y. Wu, Adsorption equilibrium of sulfur hexafluoride on multi-walled carbon nanotubes, J. Hazard. Mater. 178 (2010) 729-738.

[71] P. Orbanić, M. Fajdiga, A neural network approach to describing the fretting fatigue in aluminium-steel couplings, Int. J. Fatigue, 25 (2003) 201-207.

[72] R. Eslamloueyan, M.H. Khademi, A neural network-based method for estimation of binary gas diffusivity, Chemometr. Intell. Lab. 104 (2010) 195-204.

[73] C.S. Lee, W. Hwang, H.C. Park, K.S. Han, Failure of carbon/epoxy composite tubes under combined axial and torsional loading 1. Experimental results and prediction of biaxial strength by the use of neural networks, Compos. Sci. Technol. 59 (1999) 1779-1788.

[74] H.S. Rao, A. Mukherjee, Artificial neural networks for predicting the macromechanical behaviour of ceramic-matrix composites, Comp. Mater. Sci. 5 (1996) 307-322.

[75] M. Hojjat, S.G. Etemad, R. Bagheri, J. Thibault, Thermal conductivity of non-Newtonian nanofluids: Experimental data and modeling using neural network, Int. J. Heat Mass Tran. 54 (2011) 1017-1023.

[76] Z. Nickmand, S.F. Aghamiri, M.R. Talaie Khozanie, H. Sabzyan, A Monte Carlo simulation of the adsorption of CO_2 and SO_2 gases in pure and functionalized single walled carbon nanotubes, Sep. Sci. Technol. 49 (2014) 499-505.